Transient Interaction Between Coupling Capacitors Voltage Transformers And Transmission Lines

A. V. Carvalho Junior, *Member, IEEE*, A. R. F. Freire, and H. M. de Oliveira

***Abstract*-- Coupling capacitor voltage transformers (CCVT) are widely used in power systems and the failure of this equipment may result unexpected outages of transmission lines (TL). This study shows that switching-off shunt reactor compensated TL may lead to sustained voltage amplification in the secondary of the CCVT, the product of a transient interaction between the TL and CCVT, which causes thermal and dielectric stress to its components. This interaction is chiefly influenced by the design of the CCVT and the TL-compensation degree, as assessed by means of frequency response mappings, measurements of several parameters of different designs of CCVT, and computer simulations. Besides, this investigation presents proposals to minimize damages in the CCVT and shows digital records of the Companhia Hidro Elétrica do São Francisco (CHESF) transmission systems, which illustrate the existence of such a phenomenon.**

***Index Terms*-- CCVT, Transmission Line, TL-compensation degree, transient interaction, overvoltage.**

I. Introduction

COUPLING capacitor voltage transformers (CCVT) are widely used in power systems for monitoring, protection relays and control applications. Some electric utilities around the world have reported failures of this equipment that causes unexpected outages of transmission lines (TL), which results in severe financial penalties, damages to the CCVT and other losses [1]-[3].

Researches have been conducted to assess the performance of CCVT for electromagnetic transient response [4]-[8]. However, it is also required to analyze several other possibilities of transient interaction between the CCVT and the power system.

This work shows that the shunt compensation degree of TL (k_{sh}) has influence on its natural frequency, whereas CCVT of different designs present distinct frequency responses. Thus, during switching-off of TL, when the natural frequency of the TL approaches to the subharmonic resonant frequency of the CCVT, there are odds of sustained overvoltage occurring in their secondaries due to the ferroresonance, the result of the transitory interaction between the CCVT and the TL.

This paper is organized as follows. Section II introduces a brief approach of TL theory focused on the degree of shunt reactor compensation and its natural frequency [9]. Section III reports a review of studies carried out in a sensitive analysis to unveil the most important model parameters. Section IV outlines the frequency response tests carried out on six 230 kV different design CCVT and the measurements of relevant parameters of two of them. Section V describes the comparison between measured and simulated CCVT frequency response in order to validate the model used on digital simulations. It also presents results of TL and CCVT transient interaction by considering different degree of shunt compensation, and proposals for minimizing damages in the CCVT. Section VI shows digital recorders of the "Companhia Hidro Elétrica do São Francisco" (CHESF) transmission systems, which illustrates the existence of such a phenomenon. Conclusions are summarized in Section VII.

II. Transmission Line Features

In switching-off unloaded TL, the capacitive current is interrupted when passing zero and the voltage at this moment is closed to its maximum. That leaves different trapped voltage in the three phases due to the existing coupling between them.

When the TL is compensated by a shunt reactor, the behavior of the residual load in the capacitances may oscillate with the composition of frequencies, which depends on the compensation degree (k_{sh}) [9]. The natural frequencies of positive sequence (f_1), negative sequence (f_2) and zero sequence (f_0) are given by

$$f_1 = f_2 = \frac{1}{2\pi\sqrt{L_1 \cdot C_1}} \quad \text{e} \tag{1}$$

$$f_0 = \frac{1}{2\pi\sqrt{L_0 \cdot C_0}}, \tag{2}$$

where L_1, C_1, L_0 e C_0 are respectively the positive and zero sequency total inductances and capacitances of the circuit formed by the TL plus the shunt reactor.

The compensation reactor power (Q_l) and the capacitive reactive power of the TL (Q_c) are given by

This work was supported by the Companhia Hidro Elétrica do São Francisco (CHESF).

A. V. Carvalho Junior and A. R. F. Freire are with CHESF, 50.761-901, Recife, PE, Brazil (e-mails: ademarj@chesf.gov.br, roseval@chesf.gov.br).

H. M. de Oliveira is with the Federal University of Pernambuco, 50.740-530, Recife, PE, Brazil (e-mail: hmo@ufpe.br).

$$Q_l = \frac{U^2}{w \cdot L} \text{ e } Q_c = U^2 \cdot w \cdot C_1, \quad (3)$$

where U is the TL voltage, w is the angular frequency, and L is the inductance of the shunt reactor.

The relation between Q_l and Q_c is defined by the degree of shunt compensation (k_{sh}). To determine the oscillation frequencies, the inductance of the TL can be neglected as it is very much lesser than the value of the inductance of the reactor. Substituting the values of L and C_1 of (3) in (1) gives

$$f_1 = f_2 = \frac{1}{2\pi\sqrt{\frac{U^2}{w \cdot k_{sh} \cdot Q_c} \cdot \frac{Q_c}{w \cdot U^2}}} = \frac{1}{\frac{2\pi}{w}\sqrt{\frac{1}{k_{sh}}}} = \sqrt{k_{sh}} \cdot f, \quad (4)$$

where f is the steady-state frequency of the system. In the same way, one derives the expression of f_0

$$f_0 = \sqrt{k_{0sh}} \cdot f, \quad (5)$$

where $k_{0sh} = k_{0sh} \cdot (C_1 / C_0)$.

In the case of a total transposed compensated TL (k_{sh}=1) the discharge of the residual load occurs in the frequency equal to f with an exponential decrease, not occurring for the zero sequence. However, the lesser the k_{sh}, the greater is the difference between the system frequency and the natural frequency of the circuit formed by the TL and the shunt reactor [9]. Thus, the zero sequence mode is excited and there appears an oscillatory waveform of double frequency that is expressed by

$$u(t) = A \cdot \cos(w_1 \cdot t) + B \cdot \cos(w_0 \cdot t), \quad (6)$$

where w_1 and w_0 are the positive and zero angular frequencies and the A and B constants are the amplitudes of w_1 e w_0. From trigonometric relationships, (6) can be expressed by

$$u(t) = A\cos\left(\frac{w_0 + w_1}{2}t\right) \cdot \cos\left(\frac{w_0 - w_1}{2}t\right) + (B - A) \cdot \cos(w_0 t), \quad (7)$$

where $(B - A)$ is very small as compared with A. Thus, the final oscillation of the system comprises two frequencies, roughly calculated by

$$f_A = \frac{f_0 + f_1}{2} \text{ and } f_B = \frac{f_0 - f_1}{2}. \quad (8)$$

Table I shows to the degrees of compensation associated with oscillation frequencies f_A and f_B of CHESF's system.

TABLE I
EXAMPLES OF K_{SH} AND NATURAL FREQUENCY OF TL (CHESF)

TL	*Luiz Gonzaga – Sobradinho* (05C4)	*Milagres – Banabuiu* (04M2)
Voltage (kV)	500	230
Lenght (km)	319	225
C_0/C_1	0,5467	0,5541
Q_c (Mvar)	405,72	54,74
Q_l (Mvar)	250	10
K_{sh}	0,62	0,18
f_A (Hz)	55,40	30,05
f_B (Hz)	8,30	4,40

It is observed from Table I that, the smaller the compensation degree, the smaller is the oscillation frequency (f_A and f_B).

III. CCVT ELECTRIC MODELS

Several studies have analyzed the sensitivity of the CCVT parameters to define which one is more significant in its representation [4]-[7]. Fig. 1 shows two circuits that represent the majority of the currently commercialized CCVT. It consists of a capacitive voltage divider (C_A e C_B), a potential transformer (PT) (R_{PT1}, L_{PT1}, C_{PT1}, C_{PT12}, R_{PT2}, L_{PT2}, C_{PT2}, R_{PTm}, L_{PTm}, n_{PT}, R_{PT21}, L_{PT21}, R_{PT22}, L_{PT22}), a compensating reactor (CR) (R_{CR}, L_{CR}, C_{CR}, R_{CR1}, L_{CR1}, R_{CR2}, L_{CR2}, R_{CRm}, L_{CRm}, C_{CR}), an overvoltage protection device (PD) (PD_{PT}, PD_{CR}), a ferroresonance suppression circuit (FSC), and a drain coil (DC) (L_{DC}).

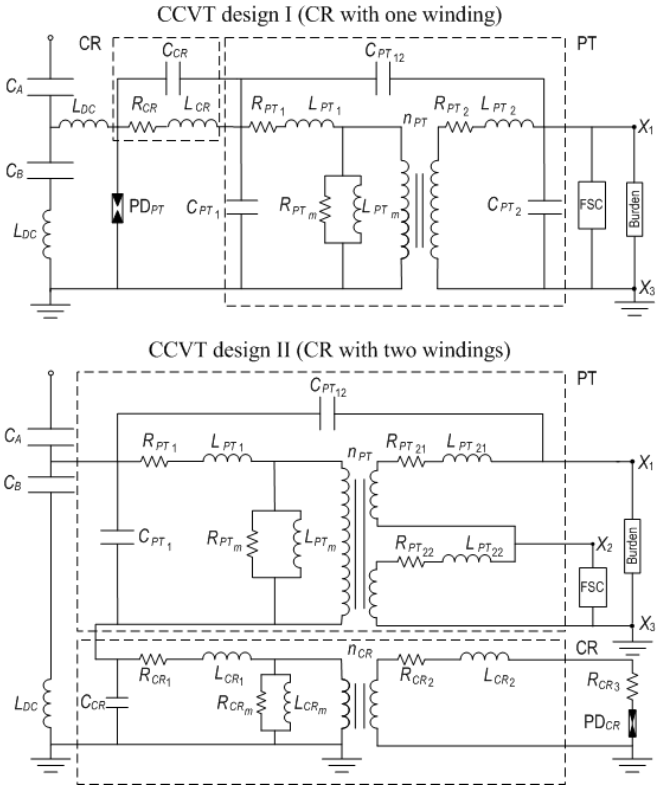

Fig. 1. General CCVT models of two different designs (CR with one and two windings).

Studies [4] and [7] adopt a rather similar circuit to the one of the CCVT of Fig. 1 (design I), where the FSC consists of a composite of a nonsaturable iron core inductor connected in parallel with a capacitor, both in series with a resistor. The circuit is tuned to the fundamental frequency with a high Q factor. The damping resistor is used so as to attenuate ferroresonance oscillations. The studies [5] and [6] used similar circuit to the one of the CCVT of Fig. 1 (design II), where the FSC is comprised by a resistance in parallel with the ensemble formed by a saturable reactor in series with a resistor. The reactor is designed to saturate before the PT and, when saturated, it inserts the in series resistance to mitigate subharmonic oscillations.

Further investigation [4]-[7] verified that the influence of the stray capacitances of the CR (C_{CR}) and the primary winding (C_{PT1}) are specially concerned at high frequencies, and the equivalent capacitance (C_e=C_A+C_B) has more

influence at lower frequencies. Moreover, the FSC should be taken into account in the CCVT model. On the other hand, parameters C_{PT1}, R_{PT2}, L_{PT2} e C_{PT2} do not play a decisive role in the CCVT frequency response.

Another analysis [6] showed that when CCVT operates with DC, the effect of the transient voltage in its secondary is substantially amplified and with slower damping. This study also had established the influence of the burden in the performance of the CCVT in transient conditions, where the absence of the burden is more susceptible to the appearance of the subharmonic ferroresonance phenomenon.

IV. Laboratory Assays

Measurements of frequency response had been carried out with six distinct CCVT with dissimilar designs and manufactures, which can be classified in two groups, similar to the circuits of Fig. 1. In the first one (namely design I), there are Type A, Type B, and Type C CCVT. In the second one (design II), there are CCVT of Type D, Type E, and Type F. The measurements were carried out for the complete CCVT, both unload and with the DC in the circuit (DC Switch opened). The signal was applied to the CCVT primary side, and the primary and secondary voltages were measured, as shown in Fig. 2.

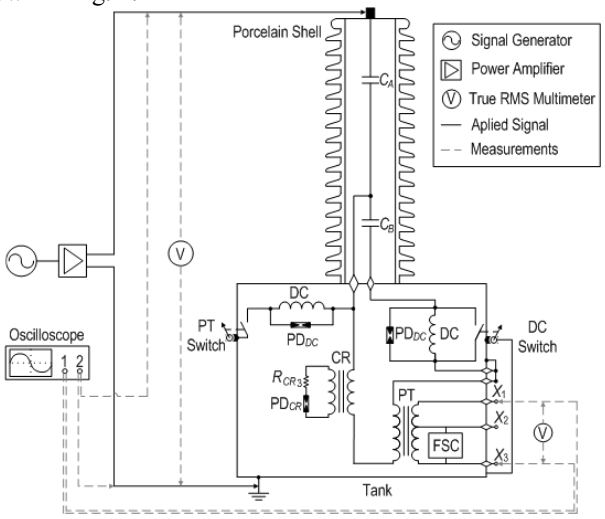

Fig. 2. Frequency response measurements.

The applied signal was varied from 5 Hz to 100 kHz, and the relation between the output voltage and the applied signal, normalized to 60 Hz, was registered. Fig. 3 and Fig. 4, respectively, present selected measurement results.

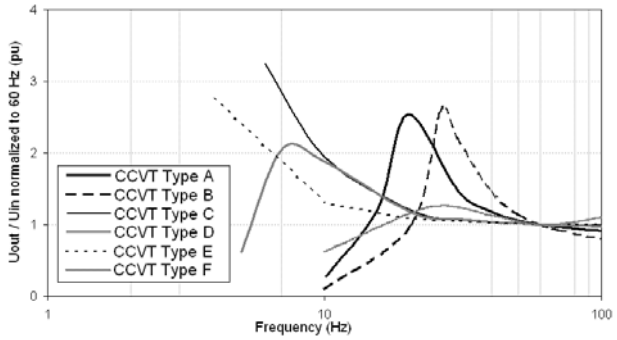

Fig. 3. CCVT Frequency Response (range 1 to 100 Hz).

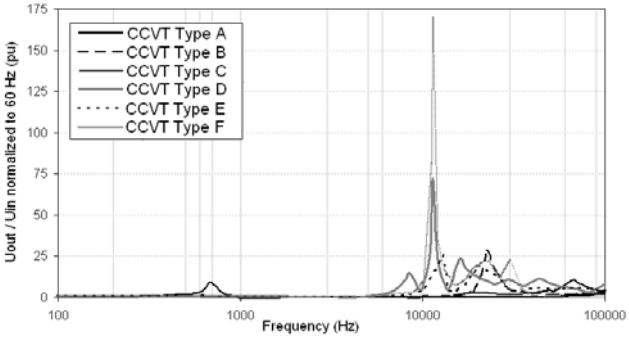

Fig. 4. CCVT Frequency Response (range 100 Hz to 100 kHz).

The frequency response performance of the CCVT differs significantly one from the other. Thus, a suitable digital simulation model must be specific for each single design and for a specific frequency bandwidth.

All CCVT present amplification of the secondary voltage for subharmonic frequencies (Fig. 2), and also for frequencies beyond 10 kHz (Fig. 3). In the first case, the amplification peaks of the secondary voltage occur between 4 and 30 Hz, and the amplitude can even surpass 3 pu. For frequencies in the range 10 to 30 kHz, amplification reaches almost 175 pu. In this case, there is an interaction between total capacitance (C_T=C_A//C_B) and L_{DC}. Thus, amplification is eliminated when the DC Switch is closed. Table II shows the measurements results of measurements carried out with opened/closed DC Switch.

TABLE II
Measurements with Opened and Closed DC Switch

CCVT	f (kHz)	U_{out} / U_{in} normalized to 60 Hz (pu) with DC Switch opened	U_{out} / U_{in} normalized to 60 Hz (pu) with DC Switch closed
Type B	22.50	28.4	0.47
Type D	11.35	72.3	0.40
Type F	11.30	170.1	0.54
Type C	19.20	2.8	0.86
Type E	13.03	25.0	0.88

CCVT Type A was not included in Table II because there is no DC component there. In this case, the amplification of the secondary voltage between 10 and 30 kHz does not occur. These results corroborate that one found in [6].

In order to analyze the transient interaction between the

CCVT and the TL, both Type A and Type D CCVT have been selected. The first one has similar circuit to the CCVT Design I (Fig. 1) and its FSC is composed of a resistance (R_{FSC}) in parallel with a reactor (L_{FSC}). The second one has similar circuit to the CCVT Design II (Fig.1), and its FSC is composed of a resistance (R_{FSC}) in parallel with a set formed by a saturable reactor (L_{FSC}) in series with a resistance (R_{FSCI}). In order to assess the parameters of these CCVT, measurements were carried out in C_A and C_B (capacitance and dissipation factor), and in PT and CR (saturation curve, resistance, ratio, and short-circuit tests).

The values of C_{PTI} and C_{CR} of both CCVT were estimated in such a way that the simulated frequency response approached to the measured frequency response up to 1 kHz. The protection devices of the two CCVT (PD_{PT} and PD_{CR}) are encapsulated spark-gaps. The PD_{PT} rated voltage is 11,5 kV_{rms}, with average disruptive voltage of 29 kV_{rms}. The disruptive voltage of PD_{CR} was estimated as 275 V_{peak}. CCVT parameter values are listed in the Appendix.

V. Digital Simulations of the Transmission System

In order to validate the models adopted for the CCVT, simulations of frequency response were carried out on the Alternative Transients Program (ATP) [10]. Fig. 5 and Fig. 6 show the results of the measured and simulated curves for both kinds of CCVT.

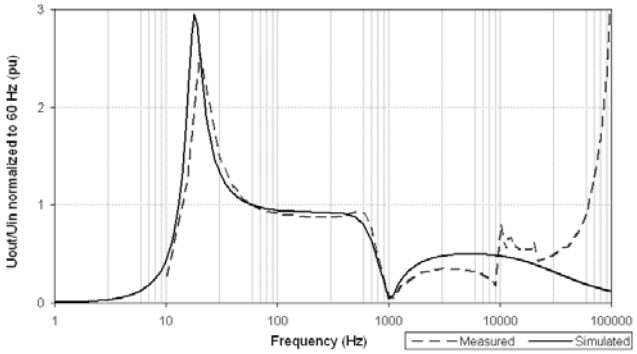

Fig. 5. Simulated and measured frequency response of Type A CCVT.

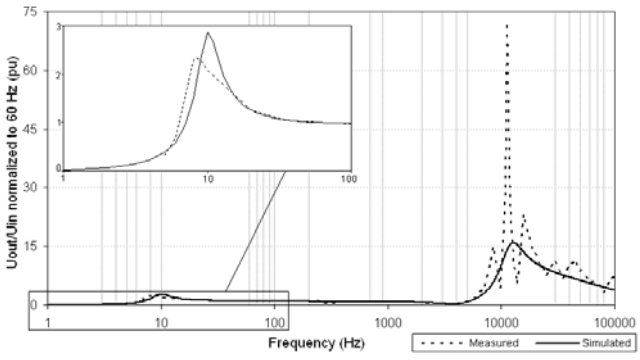

Fig. 6. Simulated and measured frequency response of Type D CCVT.

The simulation results present satisfactory agreement with the measurements found for both CCVT models, at least up to 1 kHz. Therefore, the models can be taken as adequate to examine the possible CCVT-TL interaction during low frequency oscillations, around the fundamental frequency. The greatest difference between the measurements and simulations up to 1 kHz are 13% and 19% for Type A and Type B CCVT, respectively.

The values of C_{PTI} and C_{CR} have major influence in high frequencies so their values must be adequately chosen to assess the CCVT performance at this frequency range.

A. Switching of TL with different K_{sh}

Fig. 10 presents the transmission system investigated in the digital simulations of switching-off 230 kV transmission line (TL 04M2) between *Milagres* (AIS MLG) and *Banabuiú* (AIS BNB) substations.

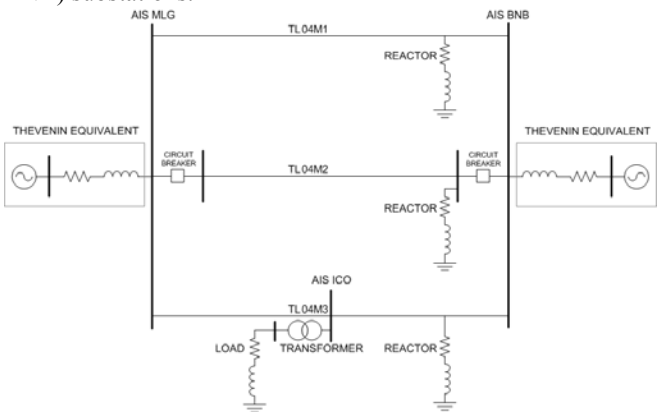

Fig. 7. Transmission system adopted in the digital simulations.

The Thevenin equivalents, represented in the *Milagres* and *Banabuiú* buses, were obtained from a short-circuit program, based on fundamental frequency (60 Hz). The solidly grounded shunt reactor has rated voltage of 230 kV, rated power of 10 Mvar, and approximately X/R of 2000. A step-down transformer of 230/69, star-delta, rated power of 100 MVA, is connected to the bus of the *Icó* substation (AIS ICO). The circuit breakers of the TL 04M2 are represented as an ordinary switches in the ATP. The amplitude and angles of the equivalents sources and the load in the 69 kV bus of substation *Icó* had been adjusted to reproduce the maximum voltage profile as well as the load flow in a typical average load condition, that corresponds to a voltage of 1,05 pu in *Icó* substation with an load flow of 40.6 MW - j39.2 Mvar in the TL 04M2, flowing from *Milagres* substation. The appendix contains the main parameters of this system.

In order to evaluate the weight of the compensation degree of TL, simulations assumed a normal opening of the TL 04M2 with compensations of 5, 10 and 20 Mvar. In all the cases, the circuit breaker of *Milagres* substation opens first, at t=100 ms, followed by a transfer trip to *Banabuiú* substation, that opens after 20 ms, in t=120 ms. The results have been checked out from *Milagres* substation terminal.

The natural frequencies of the TL 04M2 are calculated through (4) and (5), yielding 21.3 Hz, 30 Hz and 42.5 Hz for the compensation of 5, 10 and 20 Mvar, respectively.

Fig. 8 and Fig. 9 show the performance of the CCVT Type A and Type B, respectively. The secondary voltage of the CCVT was multiplied in each and every one case by the rated ratio to represent the value in the transmission line. The results showed in all figures are those concerning the phase B.

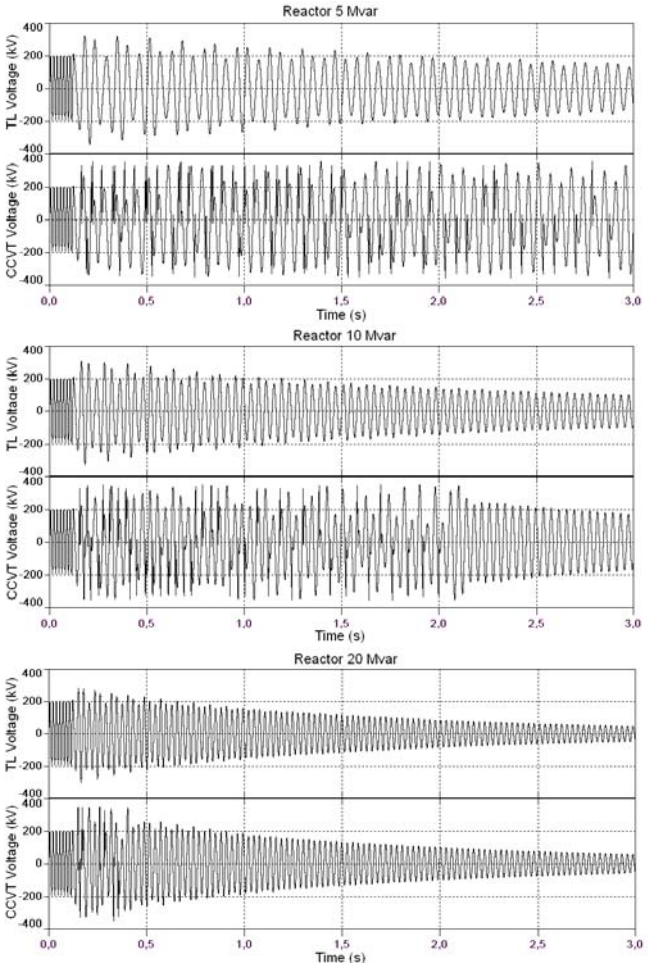

Fig. 8. TL and Type A CCVT Voltages found by ATP simulation.

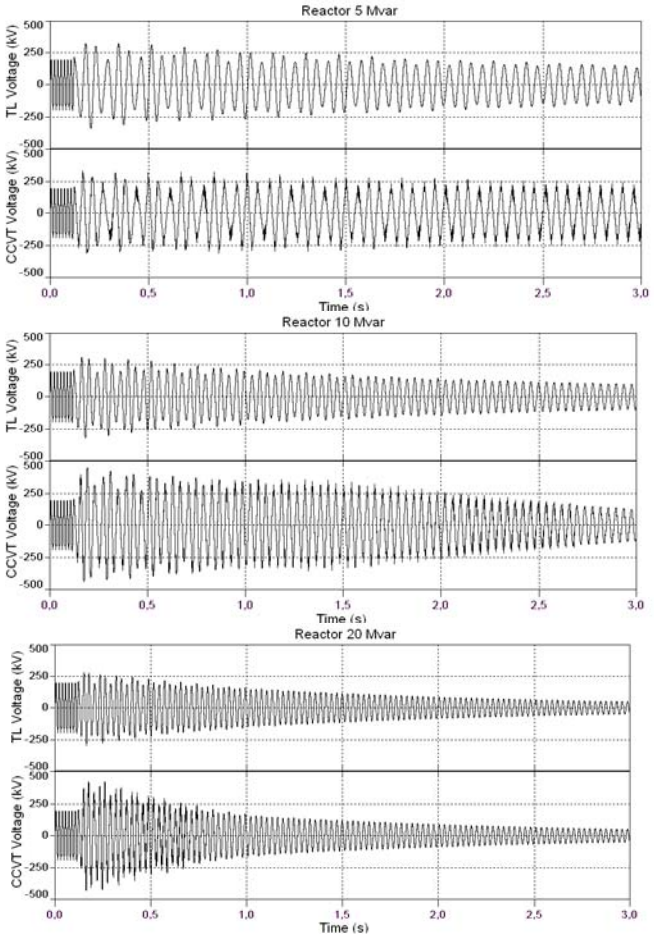

Fig. 9. TL and Type D CCVT Voltages found by ATP simulation.

Fig. 8 furnishes evidences that the lesser is the degree of compensation of TL, the lesser the natural frequency of the TL, while the greater is the voltage amplifications in the secondary of the Type A CCVT, due to the approaching of its subharmonic resonant frequency.

Fig. 9 shows that the major voltage amplification in the secondary of the Type D CCVT does not occur at low degree of compensation of TL (reactor of 5 Mvar). This fact can be accounted by the nonlinearity of L_{FSC} that presents different levels of saturation for each natural frequency and voltage amplitude, which depend on the degree of compensation of TL. In this way, for compensation of a 5 Mvar, the increase of the overvoltage along with the reduction of the natural frequency results in the reactor running in a point of the saturation curve in such a way to reduce the secondary voltage. In this case, the different frequencies and voltages turns the analyses of these nonlinear circuits more complex, as in the case of the reactor of the FSC of Type D CCVT. For Type A CCVT, the reactor is considered to be linear.

B. Influence on the CCVT performance due to its components damage

If the overvoltages imposed by the power system are great enough to damage the resistor of FSC, the secondary voltage of the CCVT changes. Fig. 10 and Fig. 11 show, respectively,

the performance of the Type A and Type D CCVT without R_{FSC} and R_{FSC1} for switching-off of the TL with compensation of 10 Mvar.

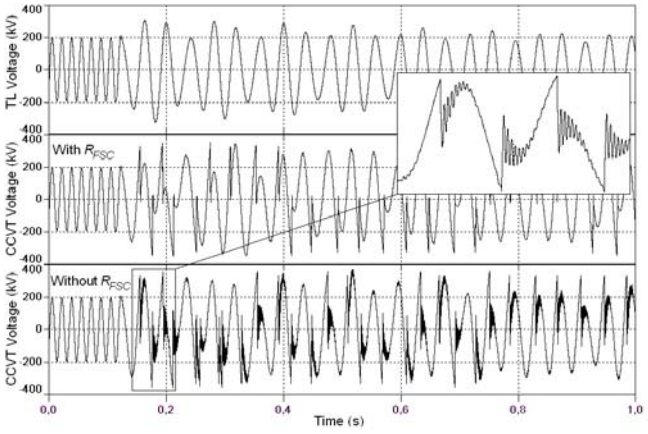

Fig. 10. Performance of Type A CCVT with damage in R_{FSC}.

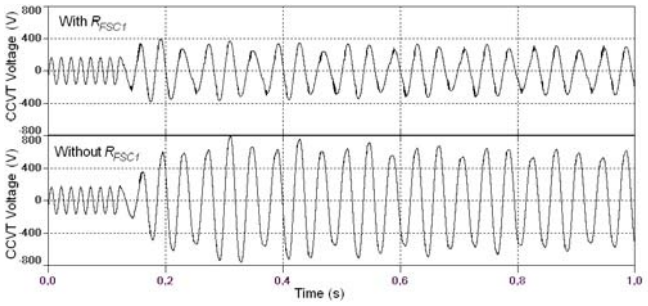

Fig. 11. Performance of Type D CCVT with damage in R_{FSC1}.

With the damage of R_{FSC}, after the spark-gap triggered, high frequency components appear in the secondary voltage of Type A CCVT, and with a damaged of R_{FSC1}, the amplification of the secondary voltage of Type D CCVT substantially increases.

C. Proposal to improve the CCVT performance

Fig. 12 shows the performance of Type A and Type D CCVT when the original spark-gap (PD_{PT} and PD_{CR}) is substituted by *ZnO* arresters, with rated burden (400 VA), and by considering the switching-off of the 04M2 TL with compensation of 10 Mvar. The data of the *ZnO* arresters can be found in the Appendix.

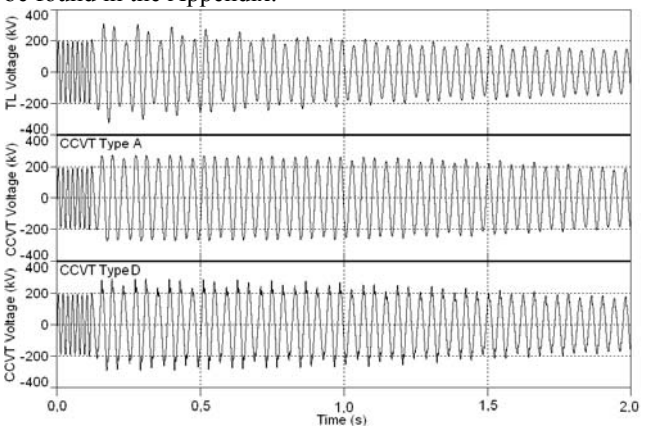

Fig. 12. Performance of Type A and Type D CCVT with *ZnO* and rated burden.

The *ZnO* arrester eliminates the fast break-down voltage engendered by the original spark-gap. Burdens in the secondary circuit help the FSC of the CCVT to suppress the ferroresonance effect, thereby decreasing the dissipated energy in its components, contributing so with the error reduction of the secondary voltage.

VI. Oscillographic Records of CHESF's Power System

Real digital records of the 230 and 500 kV CHESF's transmission system are presented in Fig.13 and Fig. 14, respectively. Fig. 13 shows the waveform occurring in the CCVT of *Milagres* substation during switching-off of TL 04M2 with compensation of 10 Mvar. This is the same TL used in the digital simulations.

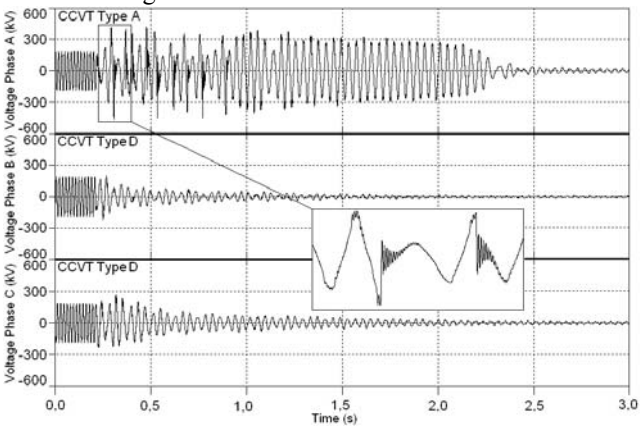

Fig. 13. Oscillographic records of switching-off TL 04M2 (CHESF).

There is a sustained overvoltage for approximately 2 seconds in the CCVT, with strong indications of damages in the R_{FSC} , similar to that one obtained in the simulation shown in Fig. 10.

Fig. 16 presents two records of the CHESF's 500 kV TL (TL 05C4) between *Luiz Gonzaga* and *Sobradinho* substations. The first one shows the voltage for switching-off the TL 05C4 with reactors of 150 Mvar in the *Luiz Gonzaga* substation and 100 Mvar in the *Sobradinho* substation (k_{sh}=62%). The second one shows the same switching-off, however without reactors in the *Luiz Gonzaga* substation (k_{sh}=25%). The records are seen by the CCVT in *Luiz Gonzaga* substation.

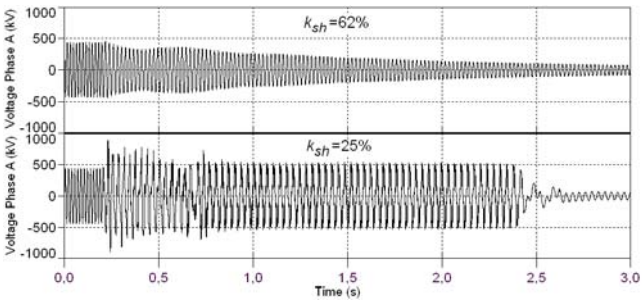

Fig. 14. Oscillographic records of switching-off TL 05C4 (CHESF).

This case offers a piece of evidence on the abrupt difference in performance of the same CCVT, showing the influence of the degree of compensation of TL in the transient interaction between the CCVT and the TL.

VII. Conclusions

This paper demonstrates the possibility of transient interaction occurring between a CCVT and a shunt compensated transmission line. This interaction may cause stress to the components of the CCVT, whose severity depends on the degree of compensation of the TL and the own design of the CCVT.

The majority of the CCVT operates with tiny burden when compared with its rated value. This occurs because of the evolution of the protection apparatus with digital technology, which implies in an increase of the energy dissipated by the resistances of the FSC. This may produce overheating in the oil insulation with formation of bubbles which, associated with sustained overvoltages, can result in failure of the equipment. Therefore, the CCVT should operate with nominal burden to get better performance and minor stress on its components during the transient interaction with the TL.

Manufacturers should supply the CCVT with accessible points for connections of the FSC components so as to allow the checking of their state. Moreover, to progress in the performance evaluation of the CCVT in the interaction with the transmission systems, manufacturers should also supply the equivalent circuit of the CCVT, giving the values of the parameters, which includes saturation curves of the nonlinear elements. They should also provide the frequency response up to 1 MHz with the DC Switch opened and closed.

VIII. Appendix

TABLE III
Flux and Current in The Magnetizing Branch of Transformer

Current (A_{peak})	Flux (V.s)
0.522554797	498.137515
4.48599515	547.951267
22.6326143	597.765018
264.370386	697.392521

TABLE IV
transformer, Reactor and Load

	Transformer (69 kV)	(230 kV)	Reactor (230 kV)	Load (69 kV)
R (Ω)	0.09	0.34	2.645	182.89
X (Ω)	9.1918	34.041	5290	25.10

TABLE V
Transmission Lines

	MLG–BNB (04M1)	(04M2)	MLG–ICO (04M3)	ICO–BNB (04M3)
r_1 (Ω/km)	0.097	0.087	0.0868	0.087
l_1 (mH/km)	1.379	0.977	0.943	0.943
c_1 (nF/km)	8.461	12.194	12.488	12.488
r_0 (Ω/km)	0.4111	0.390	0.372	0.375
l_0 (mH/km)	3.640	3.254	3.208	3.205
c_0 (nF/km)	6.153	6.756	6.671	6.679
λ (km)	225.900	225.100	102	123.100

TABLE VI
Thevenin Equivalents

	AIS MLG	AIS BNB
R_1 (Ω)	1.426	5.3471
X_1 (Ω)	12.485	31.716
R_0 (Ω)	0.6538	4.5018
X_0 (Ω)	9.2342	34.996
Uth (pu)	1.0237	1.0237

TABLE VII
ZnO Residual Voltage in kV peak at a 30/60 μs current

ZnO to Type A CCVT (U_{rated}=17,5 kV) Current (A_{peak})	Residual Voltage (kV_{peak})	*ZnO* to Type B CCVT (U_{rated}=20 kV) Current (A_{peak})	Residual Voltage (kV_{peak})
125	36.3	125	41.5
250	37.5	250	42.9
500	38.8	500	44.3

TABLE VIII
Flux and Current Adopted in the Model of Type A CCVT

PT of Type A CCVT Current (A_{peak})	Flux (V.s)
0.00343	73.535
0.00467	77.654
0.00588	81.426
0.00791	84.851
0.79071	1966.053

TABLE IX
Flux and Current Adopted in the Model of Type D CCVT

Type D CCVT PT Current (A_{peak})	Flux (V.s)	FSC Current (A_{peak})	Flux (V.s)
0.00420	96.691	1.33700	0.265
0.00544	108.063	1.72886	0.303
0.02622	128.954	2.61222	0.343
0.05653	147.691	8.74420	0.386
5.65274	3513.430	874.42039	7.466

TABLE X
Parameters of Type A and Type D CCVT.

Type A CCVT Parameter	Value	Type D CCVT Parameter	Value
C_A (pF)	4050	C_A (pF)	4321
C_B (pF)	42138	C_B (pF)	38820
C_{PT1} (pF)	149.70	C_{PT1} (pF)	200
C_{CR} (pF)	144.78	C_{CR} (pF)	1500
L_{PT1} (H)	4.68	L_{PT1} (H)	6.93
L_{PT2} (mH)	0.143	L_{PT21} (mH)	0.0268
L_{CR} (H)	159.57	L_{PT22} (mH)	0.0368
R_{PT1} (Ω)	446	L_{CR1} (H)	1.32
R_{PT2} (Ω)	48.50	L_{CR2} (mH)	3.56
R_{BC} (Ω)	608	L_{DC} (mH)	45

R_{PRTPI} (Ω)	68.80	R_{PT1} (Ω)	343
R_{PTm} (MΩ)	8.86	R_{PT21} (mΩ)	8.60
n_{PT} (X1-X3)	100.50	R_{PT22} (mΩ)	11.80
R_{FSC} (Ω)	186	R_{CR1} (Ω)	382
L_{FSC} (H)	0.354	R_{CR2} (Ω)	5.64
-	-	R_{CR3} (Ω)	24.80
-	-	R_{PTm}(MΩ)	11.20
-	-	R_{CRm} (MΩ)	1.26
-	-	n_{PT} (X1-X3)	116.13
-	-	n_{CR}	19.23
		R_{FSC} (Ω)	74.60
		R_{FSCJ} (Ω)	2.10

IX. Acknowledgment

This activity has been supported by Companhia Hidro Elétrica do São Francisco (CHESF) to whom the authors are grateful for providing the CCVT units and the high voltage laboratory structure. HMdO thanks the Brazilian National Council for Scientific and Technological Development (CNPq) for partial grant.

X. References

[1] V. L. C. Soares, B. T. Meyer, O. J. Rothstein, L. E. Loch, and V. V. Coelho, "Aspects of Transient Performance of CCVT in Substations," (In Portuguese), in *Proc. 2005 National Seminar on Production and Transmission of Electrical Energy*, Curitiba, Brazil.

[2] A. Villa, Z. Romero, "Failure Analysis of CVT from Substations el Tablazo and Cuatricentenario up 400 kV," in *Proc. 2005 International Conference on Power Systems Transients*, Montreal, Canada.

[3] H. M. Moraes and J. C. A. Vasconcelos, "Overvoltages in CCVT During Switching Operations," (In Portuguese), in *Proc. 1999 National Seminar on Production and Transmission of Electrical Energy*, Foz do Iguaçu, Brazil.

[4] D. Fernandes Jr, W. L. A. Neves, J. C. A. Vasconcelos, and M. V. Godoy, "Comparisons Between Lab Measurements and Digital Simulations for a Coupling Capacitor Voltage Transformer," in *Proc. 2006 IEEE Transmission & Distribution Conf. and Exp.,* pp. 1-6.

[5] D. A. Tziouvaras, P. McLaren, G. Alexander, D. Dawson, J. Ezstergalyos, C. Fromen, M. Glinkowski, I. Hasenwinkle, M. Kezunovic, Lj. Kojovic, B. Kotheimer, R. Kuffel, J. Nordstrom, and S. Zocholl, "Mathematical Models for Current, Voltage and Coupling Capacitor Voltage Transformers," *IEEE Trans. Power Delivery*, vol. 15, no. 1, pp. 62-72, Jan. 2000.

[6] M. R. Iravani, X. Wang, I. Polishchuk, J. Ribeiro, and A. Sarshar, "Digital Time-Domain Investigation of Transient Behaviour of Coupling Capacitor Voltage Transformer," *IEEE Trans. Power Delivery*, vol. 13, no. 2, pp. 622-629, Apr. 1998.

[7] M. Kezunovic, Lj. Kojovic, V. Skendzic, C. W. Fromen, D. R. Sevcik, and S. L. Nilsson, "Digital Models of Coupling Capacitor Voltage Transformers for Protective Relay Transient Studies," *IEEE Trans. Power Delivery*, vol. 7, no. 4, pp. 1927-1935, Oct. 1992.

[8] M. Graovac, R. Iravani, X. Wang, and R. D. McTaggart, "Fast Ferroresonance Suppression of Coupling Capacitor Voltage Transformers," *IEEE Trans. Power Delivery*, vol. 18, pp. 158-163, Jan. 2003.

[9] A. D'Ajuz, C. S. Fonseca, F. M. S. Carvalho, J. Amon Filho, L. E. N. Dias, M. P. Pereira, P. C. V. Esmeraldo, R. Vaisman, and S. O. Frontin, *Electrical Transients and Insulation Coordination: High Voltage Power Systems Application*, (In Portuguese). Niteroi: Fluminense Federal University - EDUFF, 1987, pp. 74-79.

[10] Leuven EMTP Center, *ATP - Alternative Transients Program - Rule Book*, Heverlee, Belgium, Jul. 1987.

XI. Biographies

Ademar Vieira de Carvalho Junior was born in Belo Horizonte, Brazil. He graduated in Electrical Engineering at Federal University of Uberlandia (UFU), Brazil, in 1999. He obtained his M.Sc. degree in Electrical Engineering at Federal University of Pernambuco (UFPE), Brazil, in 2008. Currently, he works for Companhia Hidro Elétrica do São Francisco (CHESF) as a specialist in maintenance procedures with an emphasis on testing, diagnosis and analysis of performance of Instrument Transformers from 69 to 500 kV. He represents CHESF on the Subgroup of Current Transformers of the Working Group of Substations of Eletrobras (GTMS). He has presented papers at national and international seminars (ERIAC), in addition to having had an article published in the magazine Eletroevolução of CIGRÉ Brazil. He is a member of CIGRÉ and IEEE.

Antonio Roseval F. Freire was born in Recife, Brazil. He graduated in Electrical Engineering at Federal University of Pernambuco (UFPE), Brazil, in 1985, and received his M.Sc degree from the Federal University of Rio de Janeiro (UFRJ), Brazil, in 1991. He works for Companhia Hidro Elétrica do São Francisco (CHESF) since 1985, with experience in the areas of specification, testing and performance analysis of substation equipments and static var compensators, and in the areas of electric power system operation planning and studies. He is currently a technical advisor of the CHESF department of power transmission system planning and studies. He has been an individual member of CIGRÉ since 1988.

Hélio Magalhães de Oliveira was born in Arcoverde, Brazil. He obtained both the Eng. and the M.Sc. degrees in Electrical Engineering from the Federal University of Pernambuco (UFPE), Brazil, in 1980 and 1983, respectively. Then he joined the staff of the Electronics and Systems Department of that University as a lecturer. In 1992, he obtained the "Docteur de l'Ecole Supérieure des Télécommunications" degree, in Paris, France. He was elected honoured professor by more than thirty electrical engineering undergraduate groups and often chosen as the godfather of engineering graduation ceremonies. Dr. de Oliveira authored the books Signal Analysis for Engineers: Wavelets, Rio de Janeiro: Editora Brasport, 2007 (ISBN 978-85-7452-283-8) and Fourier and Wavelet Analysis, Recife: Editora Universitária da UFPE, 2007 (ISBN 978-85-7315-417-7). His current research interests include: signal analysis, wavelets, and signal processing.